Original Research Article

Structural, Magnetic and Electromagnetic Absorption Properties of SrFe$_{11.98}$Mg$_{0.1}$Sn$_{0.1}$O$_{19}$/BaTiO$_3$ Nanocomposite Prepared by Sol- Gel Auto Combustion Method

Kamelia. Ghaffarzadeh[1], Pirouz. Derakhshi[1], Mohammad Yousefi[2]*, A. Mahmoudi[1], Parviz Aberoomand Azar[3]

[1]Department of Chemistry, Tehran North Branch, Islamic Azad University, Tehran, Iran

[2]* Department of Chemistry, Yadegar-e Imam Khomeini (RAH) Shahr-e Rey Branch, Islamic Azad University, Tehran, Iran

[3]Department of Chemistry, Science and Research Branch, Islamic Azad University, Tehran, Iran

ABSTRACT

In this research, first, nanoparticles of SrFe11.98Mg0.1Sn0.1O19 hexaferrite was synthesized via sol-gel autocombustion process and then the nanocomposites of hexagonal ferrites/perovskite with the amounts of SrFe11.98Mg0.1Sn0.1O19 /BaTiO$_3$ (50/50, 40/60, 70/30 w/w) was prepared by ball-milling method. FTIR spectra were shown that the bands at about 400 and 500 cm-1 proved the formation of hexagonal ferrites. XRD analysis was confirmed the formation of hexaferrite and perovskite phase of BaTiO$_3$. FESEM pictures was represented the formation of hexagonal nanoparticles and sphere shape of BaTiO$_3$. VSM hysteresis loop was revealed that SrFe11.98Mg0.1Sn0.1O19 belonged to the soft magnetic materials due to the 604.45Oe coercivity. By formation of nanocomposites the coercivity was increased up to 1500 Oe. VNA analysis was VNA analysis revealed that the maximum absorption of -16.4db at 11.5 GHz frequency for SrFe11.98Mg0.1Sn0.1O19 /BaTiO3 (60/40) nanocomposite. Microwave absorption properties of samples was investigated by (vector network analyzer) VNA. The maximum value of reflection loss was --16.4db at 11.5 GHz frequency for SrFe11.98Mg0.1Sn0.1O19 /BaTiO3 (60/40) nanocomposite.

Keywords: Hexaferrite, Ball- Milling, Vector Network Analyzer, Perovskite.

*Corresponding Author: Tel.: +98 (021) 55229255
E-mail: myousefi50@hotmail.com

Introduction

By using various kinds of magnetoelectronic devices, electromagnetic radiation interference results in the human health damage and disclosure of information. As the result, electromagnetic absorber materials (EMA) have been developed in recent years [1-3]. M-Type hexaferrites with high Curie temperature, high electrical resistivity and large magnetocrystalline anisotropy are perfect candidate to be used as EMA materials [4, 5]. Till now, single compounds like M-type hexaferrites can't be prosperous in fulfilling all properties that ideal EMA should have like: maximum electromagnetic attenuation, light weight and easy fabrication process, however composite materials act impressively [6]. On the other hand, for maximizing the attenuation of electromagnetic wave, the electric and magnetic parts of absorber should be matched with each other [7]. Hence, the new kinds of composites was synthesized with hexaferrites and the materials with large dielectric constant such as perovskite to maximize the attenuation of electromagnetic wave[8]. Nanocomposites with two different phases of magnetic and dielectric materials can fulfill the goal of maximum attenuation and excellent impedance matching[9-11]. For obtaining beneficial electromagnetic absorber materials, a series of nanocomposites such as $SrFe_{12}O_{19}/NiFe_2O_4$[12], $Fe–Sr_{0.8}La_{0.2}Fe_{11.8}Co_{0.2}O_{19}$[13], graphene/Strontium hexaferrite [14] and $(Ni_{0.65}Zn_{0.35}Fe_2O_4)_{0.85}$-$(BaFe_{12}O_{19})_{0.15}$[15], was synthesized. Consequently, electromagnetic properties of nanocomposites were enhanced in comparison to the pure nanoparticles. In this paper, $SrFe_{11.98}Mg_{0.1}Sn_{0.1}O_{19}$ /$BaTiO_3$ (50/50, 40/60, 70/30 w/w) nanocomposites, for comparing microwave absorption properties have been synthesized via ball- milling method. First of all $SrFe_{11.98}Mg_{0.1}Sn_{0.1}O_{19}$ was prepared by sol-gel auto combustion method. Then $BaTiO_3$ was fabricated by sol-gel method. Finally nanocomposites of $SrFe_{11.98}Mg_{0.1}Sn_{0.1}O_{19}$ /$BaTiO_3$ (50/50, 40/60, 70/30 w/w) was provided by ball- milling process. All the samples were characterized by FTIR (fourier transform infrared), XRD (x-ray diffraction), FESEM (field emission electron microscopy) and VSM (vibrating sample magnetometer) analysis. The absorption properties of each sample were investigated by VNA (vector network analyzer).

Experimental

Materials

Analytical grade of $Sr(NO_3)_2$, $Fe(NO_3)_3$, $Mg(NO_3)_2$, $SnCl_4$, $Ba(NO_3)_2$, Lucien, tetra-n-butyl titanate, citric acid, ammonium hydroxide, was used without further purification.

$SrFe_{11.98}Mg_{0.1}Sn_{0.1}O_{19}$ Synthesis

$SrFe_{11.98}Mg_{0.1}Sn_{0.1}O_{19}$ was synthesized with sol-gel autocombustion method. $Sr(NO_3)_2$, $Fe(NO_3)_3$, $Mg(NO_3)_2$, $SnCl_4$ and citric acid was dissolved in 400mL deionized water. The solution was heated up to 100°C, and then by ammonia solution adding the pH was reached to 8. Gradually the sol was ignited and converted to viscous gel. Finally, autocombustion was happened. The powder was calcined at 900°C for 5 hours[16].

$BaTiO_3$ Synthesis

0.25g barium nitrate and 0.3g Lucien was dissolved in distilled water. 0.5ml tetra-n-butyl titanate was added into the solution under vigorous stirring. The gel was obtained at 100°c and calcined at 700°c[17].

$SrFe_{11.98}Mg_{0.1}Sn_{0.1}O_{19}/BaTiO_3$ Nanocomposite Synthesis

Stoichiometric amounts of $SrFe_{11.98}Mg_{0.1}Sn_{0.1}O_{19}$ and $BaTiO_3$ was weighted and mortgaged. Certain weight ratio (50/50, 40/60, 70/30) of samples was ball- milled for 36h. The samples was dried at vacuumed oven.

Preparing Samples For Microwave Absorption

Preparation of samples for electromagnetic absorption measurements was accomplished by mixing nanocomposites with paraffin (mass ratio70/30). The samples was molded in the rectangular template with 22.86×10.16×1mm diameter and 3mm thickness.

Characterization

The phase formation was examined by X-ray diffraction (XRD) spectra with Cu-K_α radiation (λ=1.5406Å) using a XPERT-MPD Philips X-ray diffractometer with Cu K_α radiation over the

2Ө rang of 10-80° with a step rate of 5°/min. Field emission scanning electron (SIGMA, VP-500, ZEISS model), was utilized for estimating morphology of samples. The magnetic properties of samples were characterized by Lake Shore 7307 vibrating sample magnetometer. Microwave absorption in the range of X bands frequency was calculated with vector network analyzer (VNA, Agilent 8510C).

Results and Discussions

FTIR Spectra

The FTIR spectra of $SrFe_{11.98}Mg_{0.1}Sn_{0.1}O_{19}$, $SrFe_{11.98}Mg_{0.1}Sn_{0.1}O_{19}$ /$BaTiO_3$ (50/50, 40/60, 70/30 w/w) was represented at Fig1. In pure $SrFe_{11.98}Mg_{0.1}Sn_{0.1}O_{19}$ nanoparticles, the bands at 423 and 582 cm^{-1} was related to the vibration of Fe-O bond at tetrahedral and octahedral vibrations (Fig.1a) [18]. In $SrFe_{11.98}Mg_{0.1}Sn_{0.1}O_{19}$ /$BaTiO_3$ nanocomposite, besides hexaferrite vibrating modes, the new bands at 589, 590 and 592 cm^{-1} was corresponded to the vibration of Ti-O octahedron of perovskite structure(Fig.1b-d) [19].
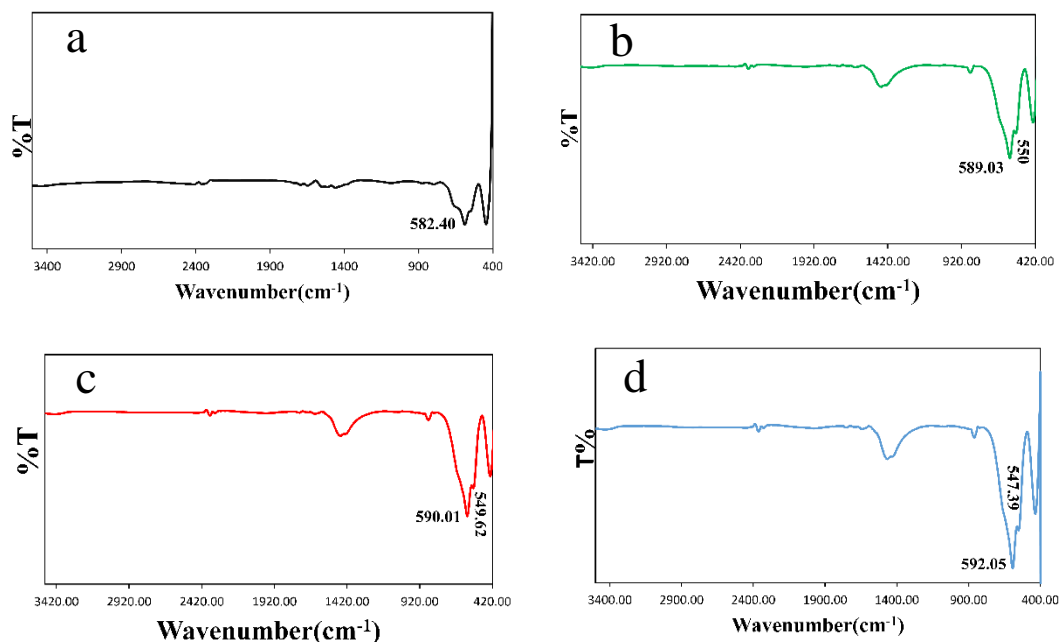

Figure 1. FTIR a) $SrFe_{11.98}Mg_{0.1}Sn_{0.1}O_{19}$, b) $SrFe_{11.98}Mg_{0.1}Sn_{0.1}O_{19}$/$BaTiO_3$ (50/50w/w), c) $SrFe_{11.98}Mg_{0.1}Sn_{0.1}O_{19}$/$BaTiO_3$ (40/60 w/w), d) $SrFe_{11.98}Mg_{0.1}Sn_{0.1}O_{19}$/$BaTiO_3$ (70/30 w/w)

XRD results

XRD patterns reveal that the formation of Strontium hexaferrite which was matched with the JCPDS number 98-004-3590. The crystallite size of particles was calculated by Scherer's equation (1):

$$D = 0.9\lambda B \cos\theta \qquad (1)$$

In which λ is the X-ray wavelength, B is the full width at half maximum and θ is the diffraction angle. The average crystallite size of $SrFe_{11.98}Mg_{0.1}Sn_{0.1}O_{19}$ was about 89nm. The peaks with Miller indices of (110),(107), (114), (108), (203), and (205) presented the formation of strontium hexagonal ferrite[20].

In $SrFe_{11.98}Mg_{0.1}Sn_{0.1}O_{19}$ /$BaTiO_3$ (50/50, 40/60, 70/30 w/w) X-ray patterns, the peaks which was related to the hexaferrite (cycles) and perovskites (stars) was appeared (fig2). These kind of X-ray patterns show that nanocomposites of hexaferrite/perovskites was synthesized successfully [21]. There was no impurities in XRD results which was represented the formation of pure nanocomposites.
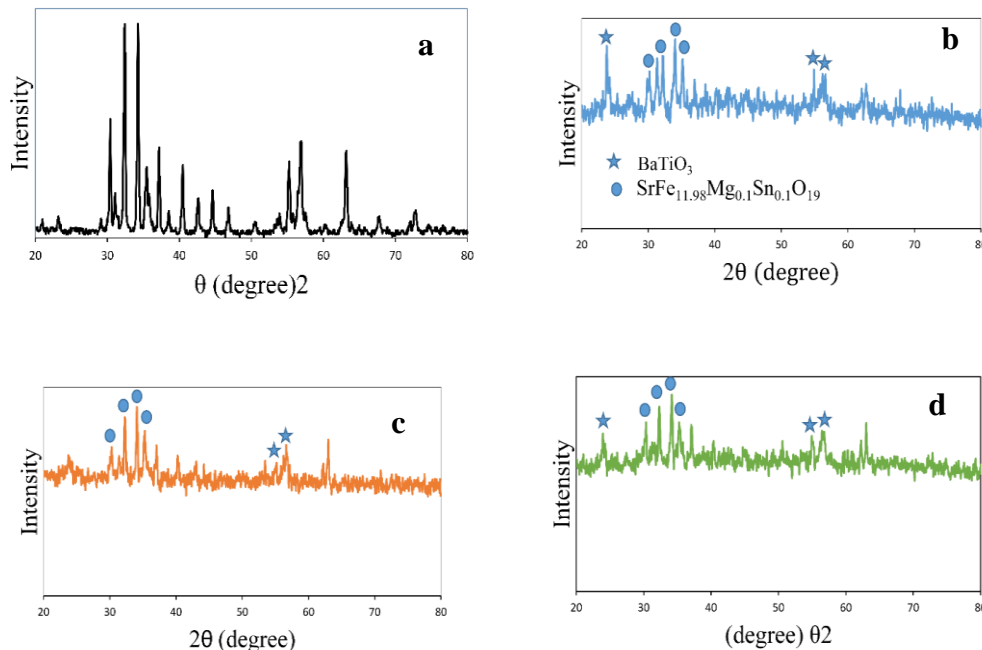

Figure 2. XRD a) $SrFe_{11.98}Mg_{0.1}Sn_{0.1}O_{19}$, b) $SrFe_{11.98}Mg_{0.1}Sn_{0.1}O_{19}$/$BaTiO_3$ (50/50w/w), c) $SrFe_{11.98}Mg_{0.1}Sn_{0.1}O_{19}$/$BaTiO_3$ d) $SrFe_{11.98}Mg_{0.1}Sn_{0.1}O_{19}$/$BaTiO_3$ (70/30 w/w)

FE-SEM pictures

FE-SEM micrographs of samples was shown at Fig3. Hexagonal platelet structure of $SrFe_{11.98}Mg_{0.1}Sn_{0.1}O_{19}$ reveals the formation of hexaferrite. In $SrFe_{11.98}Mg_{0.1}Sn_{0.1}O_{19}$ /$BaTiO_3$ nanocomposites, the sphere particles of $BaTiO_3$ and hexagonal structure of $SrFe_{11.98}Mg_{0.1}Sn_{0.1}O_{19}$ confirm the existence of nanocomposites. In all products agglomeration of samples was happened due to magnetic properties of M-type hexagonal ferrites [22-25].
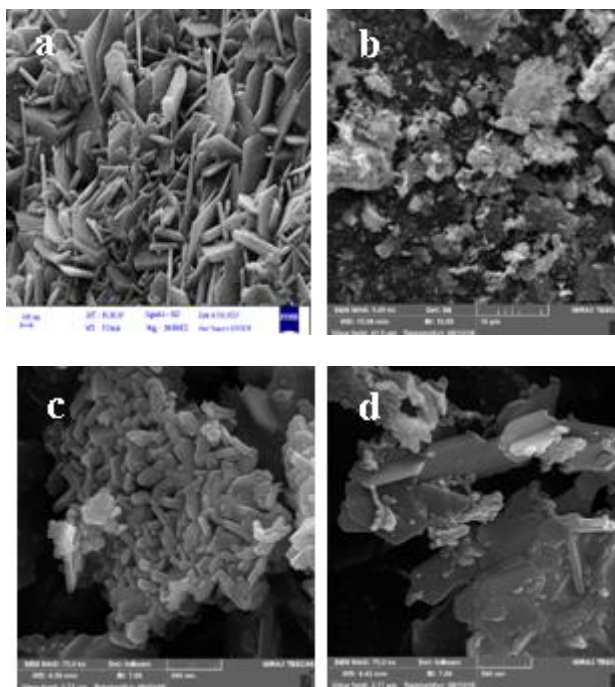

Figure3. FESEM micrograph a) $SrFe_{11.98}Mg_{0.1}Sn_{0.1}O_{19}$, b) $SrFe_{11.98}Mg_{0.1}Sn_{0.1}O_{19}$/$BaTiO_3$ (50/50w/w), c) $SrFe_{11.98}Mg_{0.1}Sn_{0.1}O_{19}$/$BaTiO_3$ (40/60 w/w), d) $SrFe_{11.98}Mg_{0.1}Sn_{0.1}O_{19}$/$BaTiO_3$ (70/30 w/w)

VSM Hysteresis Loops

Iron in the hexagonal structure occupied five different sites in tetrahedral 4f1 ($\downarrow$), bipyramidal 2b ($\uparrow$), and three octahedral sites (12 k ($\uparrow$), 4f2 ($\downarrow$), and 2a ($\uparrow$)) [26]. On the whole, 4+ cation are responsible for the magnetization properties of samples[27]. Sn^{4+} is substituted for Fe^{3+} in bipyramidal 2b and tetrahedral 4f1 sites. For more distortion, tin preferred to occupy bipyramidal 2b rather than 4f1 sites [28]. As a result, the saturation magnetization decreased in comparison to the pure strontium hexaferrite (56emu/g)[29]. In $SrFe_{11.98}Mg_{0.1}Sn_{0.1}O_{19}$/$BaTiO_3$nanocomposites by adding $BaTiO_3$, saturation magnetization reduced (39.81 to 28.83 emu/g) due to the non-magnetic properties of perovskites. In 60/40 and 70/30 nanocomposites because of the increasing

of magnetic phase (hexaferrite), the saturation magnetization increased (35.34 and 36.14 emu/g) (Fig. 4). Magnetic data of all samples was observed at table1. Coercivity of doped strontium hexaferrite was decreased (5000Oe to 604.45Oe) due to the improvement of uniaxial anisotropy along c axis.

Based on equation (2):

$$H_c = 2k / \mu_0 M_s \quad (2)$$

In which coercivity is in reverse relation with saturation magnetization. In this equation k is magnetocrystalline anisotropy constant, M_S is the saturation magnetization, μ_0 is the permeability of free space and H_c is coercivity. By decreasing saturation magnetization from 39.81 to 28.83 emu/g, the coercivity was increased from 604.45 to 1500 Oe.
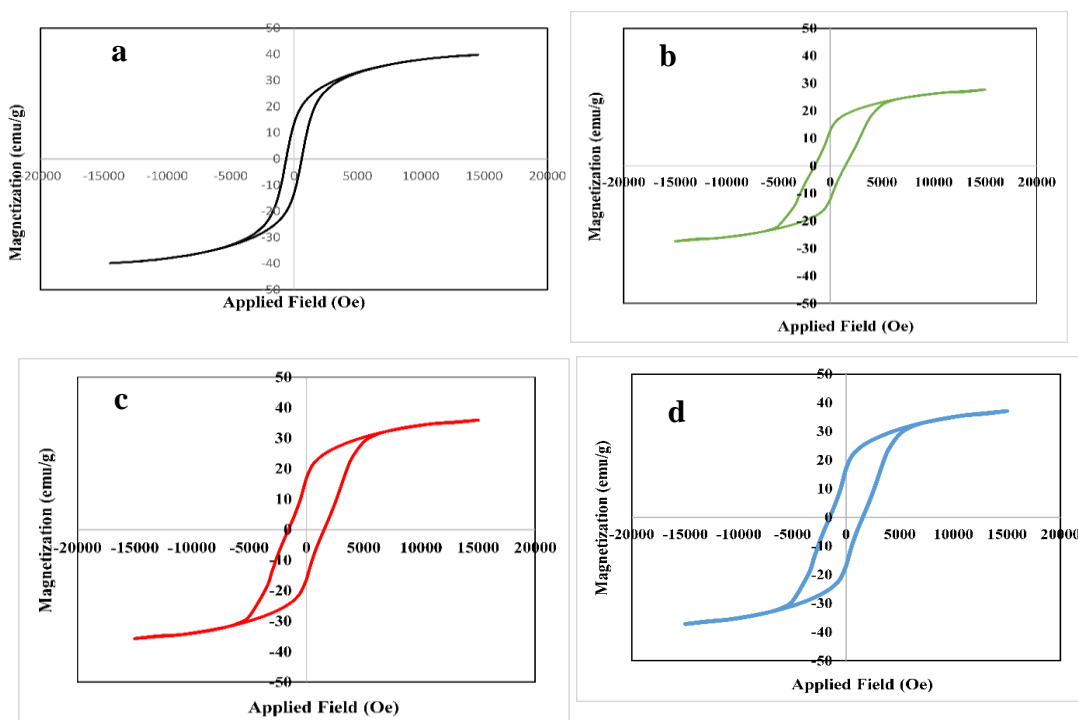

Figure 2. Hysteresis loops of a) $SrFe_{11.98}Mg_{0.1}Sn_{0.1}O_{19}$, b) $SrFe_{11.98}Mg_{0.1}Sn_{0.1}O_{19}/BaTiO_3$ (50/50w/w), c) $SrFe_{11.98}Mg_{0.1}Sn_{0.1}O_{19}/BaTiO_3$ (40/60 w/w), d) $SrFe_{11.98}Mg_{0.1}Sn_{0.1}O_{19}/BaTiO_3$ (70/30 w/w)

Table 1. Magnetic data of $SrFe_{11.98}Mg_{0.1}Sn_{0.1}O_{19}$ and $SrFe_{11.98}Mg_{0.1}Sn_{0.1}O_{19}$ /$BaTiO_3$ (50/50, 40/60, 70/30 w/w)

sample	M_s(emu/g)	M_r(emu/g)	M_r/M_s	H_c(Oe)
$SrFe_{11.98}Mg_{0.1}Sn_{0.1}O_{19}$	39.81	35.14	0.88	604.45
$SrFe_{11.98}Mg_{0.1}Sn_{0.1}O_{19}/BaTiO_3$(50/50)	28.83	23.69	0.82	1500
$SrFe_{11.98}Mg_{0.1}Sn_{0.1}O_{19}/BaTiO_3$(60/40)	35.34	32.21	0.91	1500
$SrFe_{11.98}Mg_{0.1}Sn_{0.1}O_{19}/BaTiO_3$(70/30)	36.14	32.77	0.90	1500

The sequence ratio (Mr/Ms) of all samples was calculated. Various ratio of Mr/Ms was differed each sample in different application.

Electromagnetic absorption properties

Microwave absorption properties of samples was investigated by reflection loss, and the reflection loss can be calculated by following equation based on transmission loss theory (3):

$$R(db) = 20\log\left|\frac{Z_{in}-1}{Z_{in}+1}\right|$$

$$Z_{in} = \sqrt{\frac{\mu_r}{\varepsilon_r}}\tanh\left[j(\frac{2\pi}{c})\sqrt{\mu_r\varepsilon_r}fd\right] \quad (3)$$

In these equations, Zin is the input impedance, μr is the permeability, εr is the permittivity, f is the microwave frequency, c is the light velocity, d is the thickness of absorbing layer and j is an imaginary number. The effective bandwidth describes the frequency with the reflection loss is less than -10 db[30].In $SrFe_{11.98}Mg_{0.1}Sn_{0.1}O_{19}$M-type hexaferrite, reflection loss is -4db at 8-12GHz range which reveals that the doped strontium hexaferrite shows the absorbance percentage of about 10% (Fig. 5). By adding perovskite, the reflection loss reaches to -16.4db at 11.5 GHz for $SrFe_{11.98}Mg_{0.1}Sn_{0.1}O_{19}/BaTiO_3$ 60/40 nanocomposite. In $SrFe_{11.98}Mg_{0.1}Sn_{0.1}O_{19}/BaTiO_3$ 50/50 nanocomposite, the reflection loss reaches to -16db at 12 GHz. In $SrFe_{11.98}Mg_{0.1}Sn_{0.1}O_{19}/BaTiO_3$ 70/30 nanocomposite the reflection loss reaches to -14.8db at 10.5GHz. The reports reveal that coupling dielectric loss and magnetic loss mechanism can improve the electromagnetic wave attenuation and consequently increase the reflection loss. Therefore, by adding $BaTiO_3$ to $SrFe_{11.98}Mg_{0.1}Sn_{0.1}O_{19}$, rather than magnetic loss, the dielectric loss mechanism will be occurred on the surface of the nanocomposite due to the interfacial

polarization. As a result, the reflection loss increases from -4 to -16.4db at GHz in 3mm thickness.
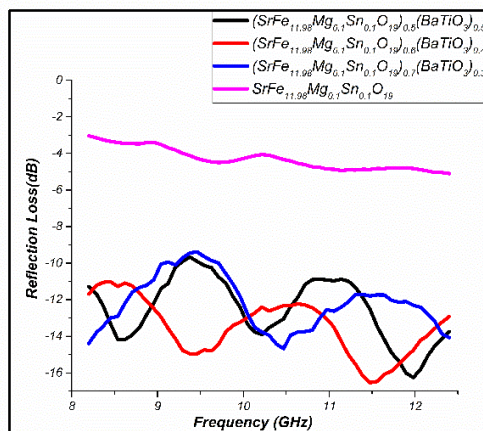

Figure 5. Reflection loss versus frequency curves of $SrFe_{11.98}Mg_{0.1}Sn_{0.1}O_{19}$ and $SrFe_{11.98}Mg_{0.1}Sn_{0.1}O_{19}/BaTiO_3$ (50/50, 40/60, 70/30 w/w)

Conclusions

The $SrFe_{11.98}Mg_{0.1}Sn_{0.1}O_{19}/BaTiO_3$ nanocomposite was synthesized successfully. FTIR spectrums approve the formation of nanocomposites. XRD results show that both phases of hexaferrite and perovskite was synthesized completely. FESEM pictures represent the hexagonal structure of $SrFe_{11.98}Mg_{0.1}Sn_{0.1}O_{19}$ and sphere shape of $BaTiO_3$. By adding perovskite phase, saturation magnetization of nanocomposites was decreased due to the reduction of magnetic hexaferrite phase. For adjusting, dielectric and magnetic parts of electromagnetic absorber, the perovskite with high dielectric properties was added to the hexaferrite. After this adjustment the reflection loss of sample was enhanced.

References

[1]　　J. Chen, *Journal of Alloys and Compounds.* 679, 335 (2016).

[2]　　X. Huang, Z. Chen, L. Tong, M. Feng, Z. Pu., X. Liu, *Materials Letters.* 111, 24 (2013).

[3]　　L. Zhang, *Polymer Degradation and Stability,* 91, 2213 (2006).

[4]　　R. C. Pullar, *Progress in Materials Science,* 57, 1191 (2012).

[5]　　H. Yanbing, J. Sha, S. Lina, T. Quan, L. Qin, J. Hongxiao, *Journal of Alloys and Compounds.* 486, 348 (2009).

[6]　　M. M. Hessien, *Journal of Magnetism and Magnetic Materials,* 320, 336 (2008).

[7]   J. Luo, Y. Xu, H. Mao, *Journal of Magnetism and Magnetic Materials.* 381: 365 (2015).

[8]   W. W. Lee, W.H. Chung, W.S. Huang, W.C. Lin, W.Y. Lin, Y. R. Jiang, *Journal of the Taiwan Institute of Chemical Engineers.* 44, 660 (2013).

[9]   S. S. S. Afghahi, M. Jafarian, *Journal of Magnetism and Magnetic Materials.* 406, 184 (2016).

[10]   Z. Sarikhani, M. Manoochehri, *Int. J. New. Chem.*,7(1),30 (2020).

[11]   G. Mahmoudzadeh, S.A. Khorrami, *Int. J. New. Chem.*,5(4),172 (2018).

[12]   M. Mehdipour, *J. Appl. Phys.*114 (2013).

[13]   Z. Zhang, *Journal of Magnetism and Magnetic Materials,* 324, 2177(2012).

[14]   Z. Durmus, H. Kavas, *Materials Chemistry and Physics.*163, 439 (2015).

[15]   B. K. G. Subhenjit Hazra, Manoj Kumar Patra, *Powder Technology.*279, 10 (2015).

[16]   S. Khorrami, F. Gharib, *Int.J.Nano.Dim.*3, 221 (2011).

[17]   M. Enhessari , *Int.J.Nano.Dim.* 2, 125 (2010).

[18]   Z. Mosleh, P. Kameli, A. Poorbaferani, M. Ranjbar, *Journal of Magnetism and Magnetic Materials,* 397, 101 (2016).

[19]   D. Sun, X. Jin, *Ferroelectrics,* 355, 145 (2007).

[20]   M. J. Iqbal, *Journal of Magnetism and Magnetic Materials,* 322, 1720 (2017).

[21]   S. Ozah., N. S. Bhattacharyya., , Development of BaAlxFe12−xO19-NPR nanocomposite as an efficient absorbing material in the X-band, *Journal of Magnetism and Magnetic Materials.*374:516 (2015).

[22]   Wang, *Journal of Alloys and Compounds,* 588, 2012 (2014).

[23] Wang, *Journal of Magnetism and Magnetic Materials*, 377,362 (2015).

[24] H. Z. Wang., B. Yao, *Journal of Alloys and Compounds,* 537, 43 (2012).

[25] J. Wang, C. Ponton , *Journal of alloys and compounds.*403,104 (2005).

[26] S. Chawla, R. Mudsainiyan , *Journal of Magnetism and Magnetic Materials* 350, 23 (2014).

[27] M. Mousavinian, A. Ghasemi, *Journal of Electronic Materials* 43, 2573 (2014).

[28] S. Ghezelbash, *IEEE Transaction on Magnetics* (2018).

[29] Sharbati, " *Solid State Communications,* 152,199 (2012).

[30] Li," *Applied Surface Science.* 258,3659 (2012).

How to Cite This Article